

# Reflectionless eigenstates of the $\text{sech}^2$ potential

John Lekner<sup>a)</sup>

School of Chemical and Physical Sciences, Victoria University of Wellington, PO Box 600, Wellington, New Zealand

(Received 23 May 2007; accepted 28 August 2007)

The one-dimensional potential well  $V(x) = -(\hbar^2\nu(\nu+1)/2ma^2) \text{sech}^2(x/a)$  does not reflect waves of any energy when  $\nu$  is a positive integer. We show that in this reflectionless case the solutions of Schrödinger's equation can be expressed in terms of elementary functions. Wave packets can be constructed from these energy eigenstates, and the propagation of such wave packets through the potential region can be studied analytically. We find that the group velocity of a particular packet can substantially exceed the group velocity of a free-space Gaussian packet. The bound states of the potential can also be expressed in terms of elementary functions when  $\nu$  is an integer. The special properties of the integer  $\nu$  potentials are associated with critical binding. © 2007 American Association of Physics Teachers.

[DOI: 10.1119/1.2787015]

## I. INTRODUCTION

It is remarkable, even amazing, that the potential well

$$V(x) = -\frac{\hbar^2}{2ma^2} \frac{\nu(\nu+1)}{\cosh^2(x/a)} \quad (1)$$

is reflectionless, *at any energy*, if  $\nu$  is a positive integer. The potential (1) (or the equivalent dielectric function profile) was first considered by Epstein<sup>1</sup> (see also Eckart<sup>2</sup>), and is treated in some quantum mechanics texts.<sup>3,4</sup> The  $\nu=1$  form of Eq. (1) appears as the simplest of a family of reflectionless profiles.<sup>5</sup>

When  $\nu$  is a positive integer, there is no reflection at any energy, and thus no reflection of any wave packet formed by superposition of positive energy eigenstates. A numerical study has reported<sup>6</sup> that Gaussian wave packets are made narrower by passage over a reflectionless  $\text{sech}^2$  well, and that they can travel faster than a free-space packet. In this paper we shall study these effects analytically, by first reducing the positive energy eigenstates to elementary form.

## II. REFLECTIONLESS POSITIVE ENERGY EIGENSTATES

For positive energies we write  $E = \hbar^2 k^2 / 2m$ , and the Schrödinger equation with potential energy given by Eq. (1) reads

$$\frac{d^2\psi}{dx^2} + \left[ k^2 + \frac{\nu(\nu+1)}{a^2 \cosh^2(x/a)} \right] \psi = 0. \quad (2)$$

The potential (1) is even in  $x$ , so parity is a good quantum number, and the two independent solutions of Eq. (2) can be taken to be the even and odd functions<sup>4</sup>

$$\begin{aligned} \psi_\nu^e(x) &= \left( \cosh \frac{x}{a} \right)^{\nu+1} F\left( \alpha, \beta; \frac{1}{2}; -\sinh^2 \frac{x}{a} \right) \\ \psi_\nu^o(x) &= \left( \cosh \frac{x}{a} \right)^{\nu+1} \sinh \frac{x}{a} F\left( \alpha + \frac{1}{2}, \beta + \frac{1}{2}; \frac{3}{2}; \right. \\ &\quad \left. -\sinh^2 \frac{x}{a} \right), \end{aligned} \quad (3)$$

where

$$\alpha = \frac{1}{2}(\nu+1+ika), \quad \beta = \frac{1}{2}(\nu+1-ika). \quad (4)$$

$F$  denotes the hypergeometric function,<sup>7</sup> which can be represented by the Gauss hypergeometric series

$$F(\alpha, \beta; \gamma; \zeta) = \frac{\Gamma(\gamma)}{\Gamma(\alpha)\Gamma(\beta)} \sum_{n=0}^{\infty} \frac{\Gamma(\alpha+n)\Gamma(\beta+n)}{\Gamma(\gamma+n)} \frac{\zeta^n}{n!} \quad (5)$$

within the unit circle  $|\zeta|=1$ . Because  $F(\alpha, \beta; \gamma; \zeta)$  is symmetric with respect to interchange of  $\alpha$  and  $\beta$ , and  $\alpha$  and  $\beta$  are complex conjugates, with  $\gamma$  and  $\sinh^2 x/a$  real,  $\psi_\nu^e$  and  $\psi_\nu^o$  are real.

When  $\nu=0$  there is no potential, so  $\psi_0^e$  and  $\psi_0^o$  are what mathematicians refer to as trivial solutions. However, their structure gives us a hint for the reduction of solutions for all integer  $\nu$ . In Eq. (15.1.18) of Ref. 7, namely

$$F\left( \alpha, 1-\alpha; \frac{1}{2}; \sin^2 z \right) = \frac{\cos(2\alpha-1)z}{\cos z}, \quad (6)$$

we set  $\alpha = \frac{1}{2}(1+ika)$ . Likewise in Eq. (15.1.16) of Ref. 7, which reads

$$F\left( \alpha, 2-\alpha; \frac{3}{2}; \sin^2 z \right) = \frac{\sin(2\alpha-2)z}{(\alpha-1)\sin 2z}, \quad (7)$$

we set  $\alpha = 1+(i/2)ka$ . In both equations we replace  $z$  by  $ix/a$ . These identities then give us the expected  $\cos kx$  and  $\sin kx$  eigenstates:

$$\psi_0^e = \cos kx, \quad \psi_0^o = \frac{\sin kx}{ka}. \quad (8)$$

The integer  $\nu$  solutions can be obtained by using Eqs. (6) and (7) and the differentiation formulas of Sec. 15.2 of Ref. 7. For example (with  $z=ix/a$  as above, and  $\nu=1$ )

$$\psi_1^e = \cos^2 z F\left( \alpha, 2-\alpha; \frac{1}{2}; \sin^2 z \right), \quad \alpha = 1 + \frac{i}{2}ka. \quad (9)$$

Using Eq. (7) and (15.2.4) with  $n=1$ , namely

$$\frac{d}{d\zeta} [\zeta^{\gamma-1} F(\alpha, \beta; \gamma; \zeta)] = (\gamma-1)\zeta^{\gamma-2} F(\alpha, \beta; \gamma-1; \zeta), \quad (10)$$

we find, after some reduction, that

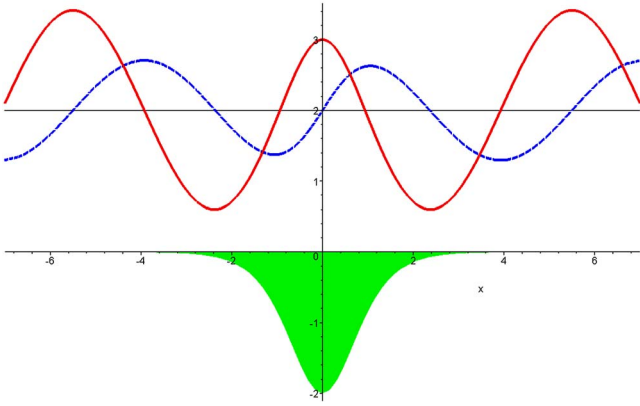


Fig. 1. The  $\nu=1$  even and odd positive energy eigenstates,  $\psi_1^e$  and  $\psi_1^o$  (Eqs. (11) and (14)), for  $ka=1$ . The wave functions are raised from the  $x$  axis to separate them from  $2ma^2/\hbar^2$  times the  $\nu=1$  potential, namely  $-2 \operatorname{sech}^2(x/a)$  (filled shape).

$$\psi_1^e = \cos kx - \tanh \frac{x}{a} \frac{\sin kx}{ka}. \quad (11)$$

Likewise (again with  $z=ix/a$ )

$$\psi_1^o = -i \cos^2 z \sin z F\left(\alpha, 3-\alpha; \frac{3}{2}; \sin^2 z\right), \quad \alpha = \frac{3}{2} + \frac{i}{2}ka. \quad (12)$$

From Eq. (7) and (15.2.3) with  $n=1$ , i.e.,

$$\frac{d}{d\zeta}[\zeta^\alpha F(\alpha, \beta; \gamma; \zeta)] = \alpha \zeta^{\alpha-1} F(\alpha+1, \beta; \gamma; \zeta) \quad (13)$$

(and using the  $\alpha \leftrightarrow \beta$  symmetry) we find

$$\psi_1^o = [1 + (ka)^2]^{-1} \left\{ ka \sin kx + \tanh \frac{x}{a} \cos kx \right\}. \quad (14)$$

The even and odd eigenfunctions for  $\nu=1$  are shown in Fig. 1.

Similarly, using Eq. (10) we can get  $\psi_2^e$  by differentiating  $\psi_1^o$ :

$$\psi_2^e = [1 + (ka)^2]^{-1} \left\{ \left[ 1 + (ka)^2 - 3 \tanh^2 \frac{x}{a} \right] \cos kx - 3ka \tanh \frac{x}{a} \sin kx \right\}. \quad (15)$$

The  $\nu=2$  odd eigenstate can be found by differentiation of  $\psi_1^e$  on using Eq. (15.2.1), which reads

$$\frac{d}{d\zeta} F(\alpha, \beta; \gamma; \zeta) = \frac{\alpha\beta}{\gamma} F(\alpha+1, \beta+1; \gamma+1; \zeta). \quad (16)$$

The result is

$$\psi_2^o = (ka)^{-1} [4 + (ka)^2]^{-2} \left\{ \left[ 1 + (ka)^2 - 3 \tanh^2 \frac{x}{a} \right] \sin kx + 3ka \tanh \frac{x}{a} \cos kx \right\}. \quad (17)$$

The even and odd eigenfunctions for  $\nu=2$  are shown in Fig. 2.

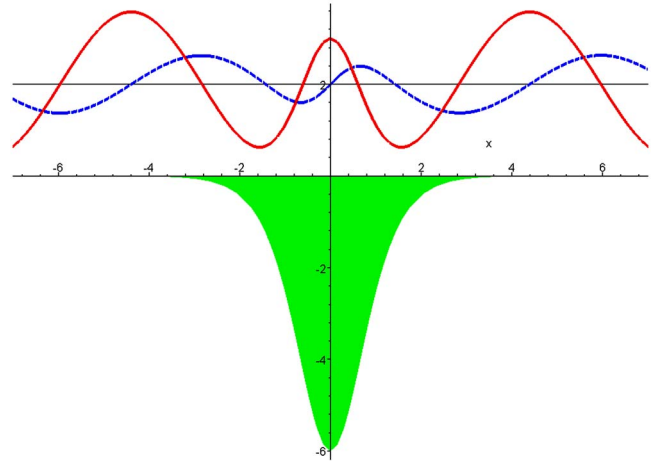


Fig. 2. The  $\nu=2$  even and odd positive energy eigenstates,  $\psi_2^e$  and  $\psi_2^o$  (Eqs. (15) and (17)), drawn for  $ka=1$ . The filled shape is  $2ma^2/\hbar^2$  times the  $\nu=2$  potential, namely  $-6 \operatorname{sech}^2(x/a)$ .

We see that the integer- $\nu$  eigenstates rapidly become more complicated as  $\nu$  increases, but they remain elementary functions, expressible in terms of  $\cos kx$ ,  $\sin kx$  and  $\tanh x/a$ .

From the even and odd eigenstates we can construct by superposition the reflectionless energy eigenstates propagating in either the  $+x$  or  $-x$  directions, for example,

$$\psi_0^+ = \psi_0^e + ika\psi_0^o = e^{ikx}, \quad (18)$$

$$\psi_1^+ = \psi_1^e + \frac{i[1 + (ka)^2]}{ka} \psi_1^o = \left[ 1 + \frac{i}{ka} \tanh \frac{x}{a} \right] e^{ikx}, \quad (19)$$

$$\psi_2^+ = \psi_2^e + \frac{ika[4 + (ka)^2]}{1 + (ka)^2} \psi_2^o = [1 + (ka)^2]^{-1} \times \left\{ 1 + (ka)^2 - 3 \tanh^2 \frac{x}{a} + 3ika \tanh \frac{x}{a} \right\} e^{ikx}. \quad (20)$$

Note that  $\psi_\nu^e$  (and thus also  $\psi_\nu^o$ ) are normalized to unity at  $x=0$ . At large  $|x|$  the modulus of  $\psi_\nu^e$  is greater than unity for  $\nu>0$ : for example,

$$|\psi_1^+|^2 \rightarrow \frac{1 + (ka)^2}{(ka)^2}, \quad |\psi_2^+|^2 \rightarrow \frac{4 + (ka)^2}{1 + (ka)^2}. \quad (21)$$

The probability flux density

$$J = \frac{\hbar}{m} \operatorname{Im} \left( \psi^* \frac{d\psi}{dx} \right) \quad (22)$$

is zero for the (real) even and odd eigenstates, and is independent of  $x$  for the  $\psi^\pm$  eigenstates, as it must be by conservation of particles:

$$J_0^+ = \frac{\hbar k}{m}, \quad J_1^+ = \frac{\hbar k}{m} \frac{1 + (ka)^2}{(ka)^2}, \quad J_2^+ = \frac{\hbar k}{m} \frac{4 + (ka)^2}{1 + (ka)^2}. \quad (23)$$

### III. CONSTRUCTION OF NONREFLECTING WAVE PACKETS

Kiriushcheva and Kuzmin<sup>6</sup> have numerically integrated the time-dependent Schrödinger equation  $H\Phi = i\hbar \partial_t \Phi$  to follow the passage of a wave packet through the  $\nu=1$  potential.

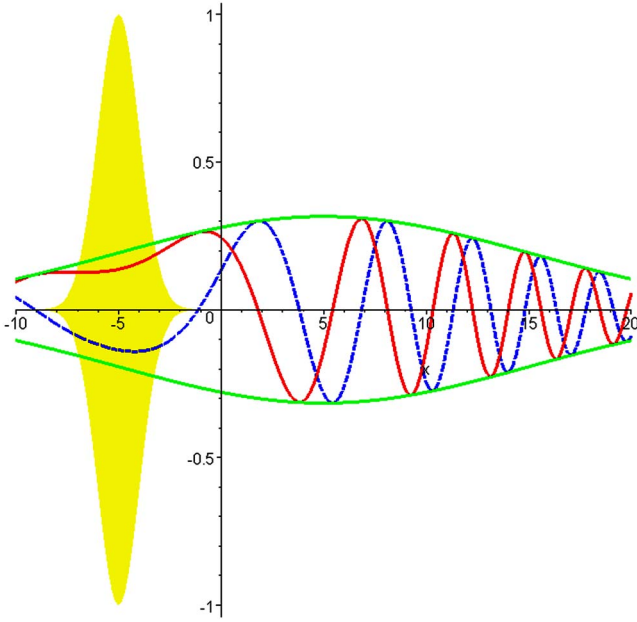


Fig. 3. The Gaussian wave packet of Eq. (25), with  $x_0 = -5b$ ,  $k_0 b = 1$  at times  $t=0$  and  $t=10b/v_0$ , where  $v_0 = \hbar k_0/m$  is the group speed. At  $t=0$  only the envelope  $\pm|\Phi_0|$  is shown. At  $t=10b/v_0$  the packet is centered on  $x=5b$ ; the envelope and the real (solid) and imaginary (dashed) parts of  $\Phi$  are shown. The packet is most compact at  $t=0$ ; at later (and earlier) times its spread is  $[b^2 + (\hbar t/m)^2]^{1/2}$ .

They reported that the packet accelerated and narrowed slightly (relative to the zero-potential case). Their wave packet was taken to be Gaussian at time zero. In the absence of a potential (in our case for  $\nu=0$ ) such a wave packet, starting at  $t=0$  centered on  $x=x_0$ ,

$$\Phi_0(x,0) = \exp\{ik_0(x-x_0) - (x-x_0)^2/2b^2\} \quad (24)$$

is known<sup>8,9</sup> to have the time development

$$\Phi_0(x,t) = \frac{b}{\sqrt{b^2 + \frac{i\hbar t}{m}}} \exp\left\{ik_0\left(x-x_0 - \frac{1}{2}v_0 t\right) - (x-x_0 - v_0 t)^2/2(b^2 + i\hbar t/m)\right\}, \quad (25)$$

where  $v_0 = \hbar k_0/m$  is the group velocity of the packet, and  $b$  gives the spatial extent of the packet at  $t=0$ . Figure 3 shows the propagation and spreading of the Gaussian packet.

The Fourier transform of Eq. (24) is

$$A_0(k) = \frac{1}{\sqrt{2\pi}} \int_{-\infty}^{\infty} dx e^{-ikx} \Phi_0(x,0) = b \exp\left\{-ikx_0 - \frac{1}{2}(k-k_0)^2 b^2\right\}. \quad (26)$$

The Fourier inverse is a superposition of free-space energy eigenstates  $e^{ikx}$ :

$$\Phi_0(x,0) = \frac{1}{\sqrt{2\pi}} \int_{-\infty}^{\infty} dx e^{ikx} A_0(k). \quad (27)$$

Since a formal solution of the time-dependent Schrödinger equation  $H\Phi = i\hbar\partial_t\Phi$  is  $\Phi(x,t) = e^{-iHt/\hbar}\Phi(x,0)$ , the time de-

pendence of the wave packet (25) is obtained from

$$\Phi_0(x,t) = \frac{1}{\sqrt{2\pi}} \int_{-\infty}^{\infty} dk e^{ikx - ik^2\hbar t/2m} A_0(k) \quad (28)$$

because each energy eigenstate, with energy  $E_k = \hbar^2 k^2/2m$ , develops in time according to the phase factor  $\exp(-iE_k t/\hbar)$ .

Our aim is to construct wave packets which solve the time-dependent Schrödinger equation in the presence of the  $\text{sech}^2$  potential. In particular, we shall use the reflectionless energy eigenstates corresponding to  $\nu=1$ :

$$\psi_1^+(k,x) = \left(1 + \frac{i}{ka} \tanh \frac{x}{a}\right) e^{ikx}, \quad E_k = \frac{\hbar^2 k^2}{2m}. \quad (29)$$

The wave packets formed by superposition of these eigenstates,

$$\Phi_1(x,t) = \frac{1}{\sqrt{2\pi}} \int_{-\infty}^{\infty} dk e^{-ik^2\hbar t/2m} \psi_1^+(k,x) A(k), \quad (30)$$

satisfy the time-dependent Schrödinger equation, for any Fourier amplitude  $A(k)$ . Because of the  $(ka)^{-1}$  term in  $\psi_1^+$ , a relatively simple wave packet is produced by taking

$$A(k) = -ikaA_0(k) = -ikab \exp\left\{-ikx_0 - \frac{1}{2}(k-k_0)^2 b^2\right\}. \quad (31)$$

This gives

$$\Phi_1(x,t) = \frac{-ib}{\sqrt{2\pi}} \int_{-\infty}^{\infty} dk e^{-ik^2\hbar t/2m} \times \left(ka + i \tanh \frac{x}{a}\right) e^{ik(x-x_0) - (k-k_0)^2 b^2/2}. \quad (32)$$

The integrals may be evaluated in terms of the Gaussian integral, since the exponent

$$-k_0^2 b^2/2 - k^2 [b^2 + i\hbar t/m]/2 + ik(x-x_0 - ik_0 b^2) \quad (33)$$

is quadratic in  $k$ . The  $ka$  term in the integrand gives the contribution

$$\begin{aligned} & \frac{ab}{\sqrt{2\pi}} e^{-k_0^2 b^2/2} \int_0^{\infty} dk k \sin kz e^{-k^2 [b^2 + i\hbar t/m]/2} \\ &= -\frac{ab}{\sqrt{2\pi}} e^{-k_0^2 b^2/2} 2\partial_z \int_0^{\infty} dk \cos kz e^{-k^2 [b^2 + i\hbar t/m]/2} \\ &= \frac{ab}{[b^2 + i\hbar t/m]^{3/2}} \exp\left(-k_0^2 b^2/2 - \frac{z^2/2}{b^2 + i\hbar t/m}\right), \\ & \quad z = x - x_0 - ik_0 b^2. \end{aligned} \quad (34)$$

The  $\tanh x/a$  term gives the contribution

$$\begin{aligned} & \tanh \frac{x}{a} \frac{b}{\sqrt{2\pi}} e^{-k_0^2 b^2/2} \int_0^{\infty} dk e^{-k^2 (b^2 + i\hbar t/m)} \cos kz \\ &= \tanh \frac{x}{a} \frac{b}{[b^2 + i\hbar t/m]^{1/2}} \exp\left(-k_0^2 b^2/2 - \frac{z^2/2}{b^2 + i\hbar t/m}\right). \end{aligned} \quad (35)$$

Thus the wave packet built up from the nonreflecting energy

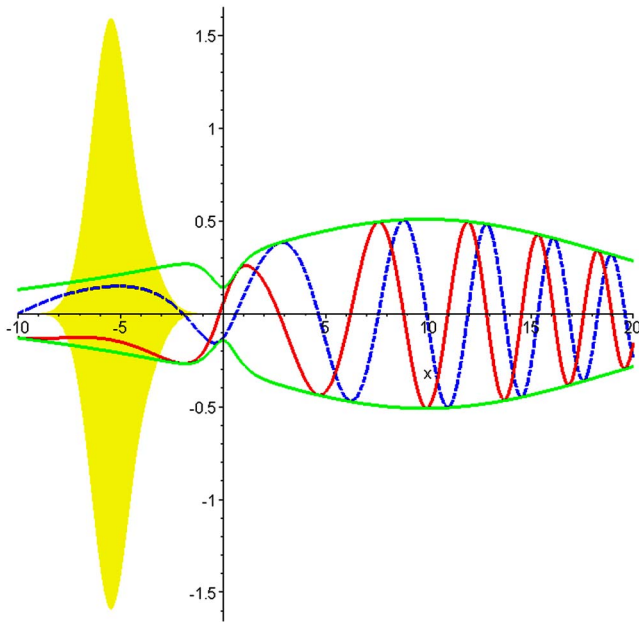


Fig. 4. The  $\nu=1$  nonreflecting wave packet of Eq. (36), drawn for  $a=b$  and otherwise using the same parameters and line types as in Fig. 3, namely  $x_0=-5a$ ,  $k_0a=1$ , at times  $t=0$  (envelope only) and  $t=10a/v_0$ . The constriction near  $x=0$  is due the potential  $-(\hbar^2/ma^2)\text{sech}^2(x/a)$  (not shown). The center of the packet is slightly to the left of  $x=-5a$  at  $t=0$ , and at about  $x=10a$  at  $t=10a/v_0$ , consistent with the group speed estimate given in Eq. (47).

eigenstates  $\psi_1^\pm(k, x)$  with Fourier amplitude given by Eq. (31) is

$$\Phi_1(x, t) = \Phi_0(x, t) \left[ \frac{a(x - x_0 - ik_0b^2)}{b^2 + i\hbar t/m} + \tanh \frac{x}{a} \right], \quad (36)$$

where  $\Phi_0$  is the free-space Gaussian wave packet given in Eq. (25). The propagation of the packet through the potential well region is illustrated in Figs. 4 and 5.

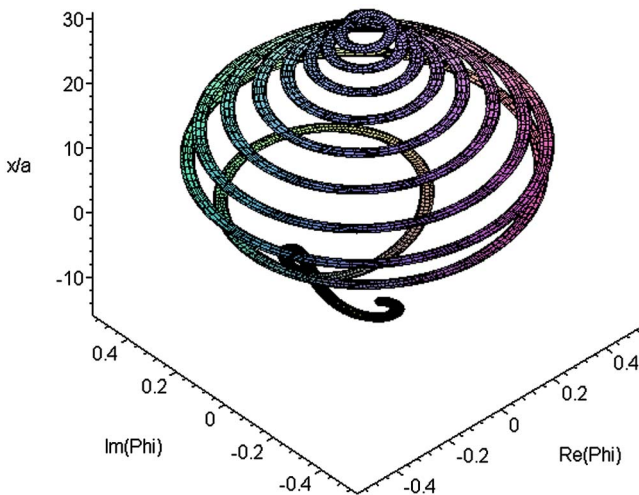


Fig. 5. Another view of the  $\nu=1$  nonreflecting wave packet, drawn as a spiral curve at  $t=10a/v_0$ , with parameters as in Fig. 4. The  $x$  axis is the direction of propagation, the transverse axes are real and imaginary parts of  $\Phi$ , also shown in Fig. 4 as solid and dashed curves, respectively.

If we take  $A(k)=A_0(k)$  in Eq. (30), a different but qualitatively similar wave packet results, namely

$$\begin{aligned} \Phi_1'(x, t) = & \Phi_0(x, t) \\ & + \sqrt{\frac{\pi b}{2a}} \tanh \frac{x}{a} e^{-k_0^2 b^2/2} \text{erfc} \left( \frac{x - x_0 - ik_0b^2}{\sqrt{2}\sqrt{b^2 + i\hbar t/m}} \right), \end{aligned} \quad (37)$$

where the complementary error function is defined by<sup>10</sup>

$$\text{erfc}(\zeta) = \frac{2}{\sqrt{\pi}} \int_{\zeta}^{\infty} d\xi e^{-\xi^2} = 1 - \frac{2}{\sqrt{\pi}} \int_0^{\zeta} d\xi e^{-\xi^2} = 1 - \text{erf}(\zeta). \quad (38)$$

We can verify by direct differentiation that the wave packets given by Eqs. (36) and (37) satisfy the Schrödinger equation with the  $\nu=1$  potential.

#### IV. GROUP VELOCITY AND WIDTH OF THE NONREFLECTING PACKET $\Phi_1(x, t)$

Kiriushcheva and Kuzmin<sup>6</sup> made a numerical study of wave packet propagation in the presence of the  $\nu=1$   $\text{sech}^2$  potential. They found that a wave packet, constructed to have the form (24) at time zero, propagated through the potential region faster than at the group speed  $v_0=\hbar k_0/m$  of the free-space Gaussian solution, and also was narrower after passing through the potential than the free-space Gaussian packet. Here we shall examine the speed and width of the  $\Phi_1(x, t)$  wave packet, given in Eq. (36).

The envelope of this packet is  $|\Phi_1(x, t)|$ , where

$$\begin{aligned} |\Phi_1(x, t)|^2 = & |\Phi_0(x, t)|^2 \left[ \tanh^2 \frac{x}{a} \right. \\ & \left. + \frac{2ab^2(x - x_0 - v_0t) \tanh \frac{x}{a} + a^2[(x - x_0)^2 + k_0^2 b^4]}{b^4 + (\hbar t/m)^2} \right] \end{aligned} \quad (39)$$

with

$$|\Phi_0(x, t)|^2 = \frac{b}{\sqrt{b^2 + (\hbar t/m)^2}} \exp \left\{ \frac{-(x - x_0 - v_0t)^2}{[b^2 + (\hbar t/m)^2]} \right\}. \quad (40)$$

The Gaussian free-space wave packet has, by inspection of Eq. (40), group speed  $v_0=\hbar k_0/m$  and width  $\sigma_0(t)=[b^2 + (\hbar t/m)^2]^{1/2}$ . The expectation values of the energy and momentum are, respectively,

$$\langle H \rangle = \frac{\hbar^2}{2m} \left( k_0^2 + \frac{1}{2b^2} \right), \quad \langle p \rangle = \hbar k_0. \quad (41)$$

To find the group speed and width associated with the wave packet  $\Phi_1(x, t)$  we limit ourselves to regions outside the potential (so that  $\tanh x/a$  takes the values  $\pm 1$ ). We differentiate  $|\Phi_1|^2$  with respect to  $x$ , and set  $x=x_0+d$ . The zeros of this derivative give the stationary points of  $|\Phi_1|^2$ . There result two cubic equations for  $d$ , corresponding to  $\tanh x/a \rightarrow 1$  and  $-1$ . There are three intrinsic speeds in the problem, namely

$$v_0 = \frac{\hbar k_0}{m}, \quad u_a = \frac{\hbar}{ma} \quad \text{and} \quad u_b = \frac{\hbar}{mb}. \quad (42)$$

At times  $t$  such that  $v_0 t$ ,  $u_a t$  and  $u_b t$  are all large compared to the lengths  $a$  and  $b$  (the range of the potential and the initial width of the free-space packet, respectively), both cubics reduce to

$$u_a^2 v_0 t^3 + (u_b^2 - u_a^2) t^2 d + v_0 t d^2 - d^3 = 0. \quad (43)$$

Equation (43) determines the position  $x = x_0 + d$  of the maximum of  $|\Phi_1|^2$  at time  $t$ . The group speed  $v$  is found by setting  $d = vt$ :

$$u_a^2 v_0 + (u_b^2 - u_a^2) v + v_0 v^2 - v^3 = 0. \quad (44)$$

When  $v_0$  is large compared to  $u_a$  and  $u_b$  (that is, at high energy expectation values),  $v \approx v_0$ , i.e., the reflectionless packet travels at about the same speed as the free-space wave packet  $\Phi_0$ . More precisely, the high-energy asymptotic form of the group speed  $v$  is

$$v = v_0 \left\{ 1 + \frac{1}{(k_0 b)^2} - \frac{a^2 + b^2}{a^2 b^4 k_0^4} + O(k_0^{-6}) \right\}. \quad (45)$$

At low energies the situation is more complicated, and the group speed can be much greater than that of the free-space packet. For example, when  $a = b$  (and thus  $u_a = u_b$ ),

$$v = v_0 \left\{ \frac{1}{(k_0 a)^{2/3}} + \frac{1}{3} + \frac{1}{9} (k_0 a)^{2/3} + O(k_0 a)^{4/3} \right\}. \quad (46)$$

At  $k_0 a = 1 = k_0 b$  we find from Eq. (44), with  $\rho = 29 + 3\sqrt{93}$ , that

$$v = \frac{v_0}{3} [(\rho/2)^{1/3} + (2/\rho)^{1/3} + 1] \approx 1.46557 v_0. \quad (47)$$

The width of the free-space Gaussian wave packet,  $\sigma_0(t) = [b^2 + (\hbar t/m)^2]^{1/2}$ , was defined by the value of  $|x - x_0 - vt|$  at which  $|\Phi_0|^2$  fell to  $1/e$  of its maximum value, that is, when the exponent in Eq. (40) decreased from 0 to  $-1$ . For the  $\Phi_1$  wave packet we shall use the same definition. The exponent of  $|\Phi_1|^2$  is  $-X + \ln F$ , where  $X = (x - x_0 - v_0 t)^2 / [b^2 + (\hbar t/m)^2]$ , and  $F$  is the content of the square bracket in Eq. (39). Outside the range of the potential the maximum of  $|\Phi_1|^2$  occurs at  $x = x_0 + vt$  where the group speed  $v$  is determined by the cubic Eq. (44). The location of the points  $x$  at which  $X - \ln F = 1$  is determined by a transcendental equation, which we shall simplify by neglecting the slowly varying  $\ln F$  term. The breadth of the wave packet, centered on  $x_m = x_0 + vt$ , is then approximately given by the points  $x_1$  at which  $X = 1$ :

$$(x_1 - x_0 - v_0 t)^2 = b^2 + (\hbar t/m)^2. \quad (48)$$

The distance  $\sigma(t)$  between  $x_1$  and  $x_m$  is then roughly

$$\sigma(t) \approx \sigma_0(t) - (v - v_0)t, \quad \sigma_0^2(t) = b^2 + (\hbar t/m)^2. \quad (49)$$

Thus when the group speed  $v$  exceeds the group speed  $v_0$  of the free-space Gaussian packet, we expect a narrower packet than the Gaussian (at the same time of propagation). The expression given in Eq. (49) is a rough estimate only, and cannot be valid when  $v - v_0 > u_b = \hbar/m b$ , since then  $\sigma(t)$  would become negative at large times.

Our results for the group speed and wave packet width are in qualitative agreement with the numerical example given by Kiriushcheva and Kuzmin.<sup>6</sup> The propagation of a nonre-

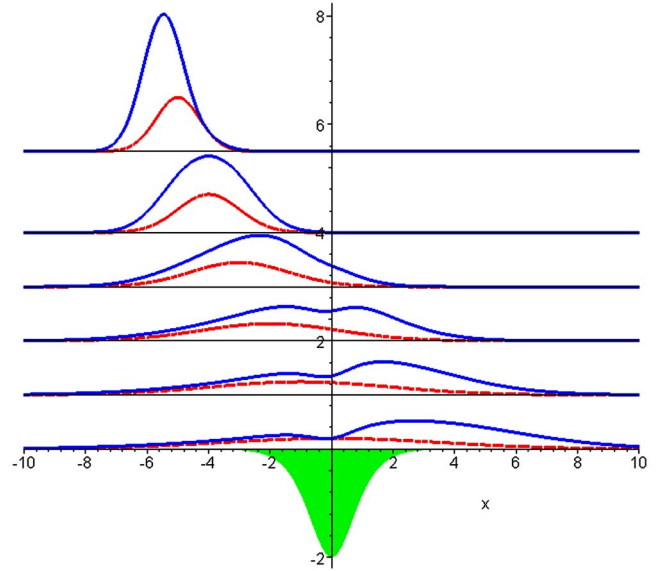


Fig. 6. Comparison of the propagation of a free-space Gaussian packet and of the  $\nu=1$  nonreflecting packet, Eqs. (25) and (36), respectively. The parameters are  $a=b$ ,  $k_0 a=1$ ,  $t=0$  (top), 1, 2, 3, 4 and  $5a/v_0$  (bottom). The potential well is also shown (shaded). The nonreflecting packet has a group speed roughly 1.5 times greater than the Gaussian. The curves show  $|\Phi_0|^2$  and  $|\Phi_1|^2$ , with  $\Phi_1$  having the larger amplitude.  $|\Phi_1|^2$  shows an indentation near  $x=0$  as it passes over the potential;  $|\Phi_0|^2$  (dashed curves) does not, because it is a free-space solution of Schrödinger's equation.

fecting packet and of a free-space Gaussian packet is illustrated in Fig. 6 for the parameter choice leading to the velocity ratio of Eq. (47).

Next we consider the question “what is so special about the integer values of  $\nu$  in Eq. (1)?”

## V. CRITICAL BINDING

The phenomenon of zero reflection of waves is common in optics, acoustics and quantum mechanics.<sup>11</sup> For example, antireflection coatings can make reflection zero at one wavelength, or very small over a range of wavelengths. What is rare is zero reflection at any wavelength. In optics and acoustics there is zero reflection by a sharp interface at the Brewster and Green angles (see, for example, Secs. 1-2 and 1-4 of Ref. 12)

$$\tan^2 \theta_B = \frac{\varepsilon_2}{\varepsilon_1}, \quad \tan^2 \theta_G = \frac{(\rho_2 v_2)^2 - (\rho_1 v_1)^2}{\rho_1^2 (v_1^2 - v_2^2)}, \quad (50)$$

where  $\varepsilon$ ,  $\rho$ ,  $v$  are dielectric constants, densities and sound speeds, respectively. The reflection of the electromagnetic  $p$  wave and of the acoustic wave is, however, zero only in the limit when the step from  $\varepsilon_1$  to  $\varepsilon_2$  or  $(\rho_1, v_1)$  to  $(\rho_2, v_2)$  is very rapid on the scale of the wavelength.

Here we have an example of a potential (or dielectric function profile) with a characteristic length  $a$ , and zero reflection for any values of  $a$  at any energy, provided  $\nu$  is an integer. Why?

The potential (1) has, for given  $\nu$ , the bound states<sup>3</sup>

$$E_n = -\frac{\hbar^2}{2ma^2}(\nu - n)^2, \quad n = 0, 1, 2, \dots, [\nu], \quad (51)$$

where  $[\nu]$  is the integer part of  $\nu$ . The Schrödinger equation for bound states, and the even and odd energy eigenstates, can be obtained from Eqs. (2) and (3), respectively, by replacing  $k$  by  $q = ik$ . The energy becomes  $-\hbar^2 q^2/2m$ . For example, for  $\nu=1$  we have the bound state

$$q = \frac{1}{a}, \quad E_0^{(1)} = -\frac{\hbar^2}{2ma^2}, \quad \psi_0^{(1)} = \operatorname{sech} \frac{x}{a} \quad (52)$$

and the just-bound (or just-unbound) state

$$q = 0, \quad E_1^{(1)} = 0, \quad \psi_1^{(1)} = \tanh \frac{x}{a}. \quad (53)$$

For  $\nu=2$  we have two bound states and one zero-energy state:

$$q = \frac{2}{a}, \quad E_0^{(2)} = -\frac{2\hbar^2}{ma^2}, \quad \psi_0^{(2)} = \operatorname{sech}^2 \frac{x}{a}, \quad (54)$$

$$q = \frac{1}{a}, \quad E_1^{(2)} = -\frac{\hbar^2}{2ma^2}, \quad \psi_1^{(2)} = \operatorname{sech} \frac{x}{a} \tanh \frac{x}{a}, \quad (55)$$

$$q = 0, \quad E_2^{(2)} = 0, \quad \psi_2^{(2)} = \operatorname{sech}^2 \frac{x}{a} - 2 \tanh^2 \frac{x}{a}. \quad (56)$$

The special property of the integer- $\nu$  potentials  $(-\hbar^2/2ma^2)\nu(\nu+1)\operatorname{sech}^2 x/a$  is that they support a *critically bound state*: one that has zero energy and a wave function of infinite range.<sup>13</sup> Systems which are near critical binding have special properties associated with the long range of the wavefunction. In three dimensions, the zero-energy scattering length  $s$  goes to infinity as the binding energy  $E$  tends to zero:<sup>3,13</sup>

$$s = \pm \left( \frac{\hbar^2}{2m|E|} \right)^{1/2} \quad (57)$$

(the positive sign is to be taken for bound states,  $E < 0$ , and the negative sign for virtual states,  $E > 0$ ). Thus systems near critical binding can be thought of as having a reach far beyond the range of the binding potential, in our case the length  $a$ . This is one reason for the nonreflecting integer- $\nu$   $\operatorname{sech}^2$  potentials. Another is the  $V(-x) = V(x)$  symmetry of the potential: as shown in Ref. 11, reflection amplitudes of symmetric profiles automatically have coincident zeros of their real and imaginary parts, whereas general profiles do not.

The above association between critical binding strengths of the  $\operatorname{sech}^2$  potentials and zero reflection adds a physical heuristic to the mathematical explanation of supersymmetric quantum mechanics. In the latter the potentials (1) and, with integer  $n$ ,

$$\frac{-\hbar^2}{2ma^2}(\nu - n)(\nu - n + 1)\operatorname{sech}^2 \frac{x}{a} \quad (58)$$

are shown to be partners in supersymmetric algebra.<sup>14</sup> If one of the partners has zero reflection amplitude they all do (Ref. 14, Eq. (3.32)). When  $\nu$  is an integer one of the potentials will be zero, and a null potential does not reflect, so all the integer- $\nu$  potentials are nonreflecting.

## VI. SUGGESTED PROBLEMS

1. Is it true in general that symmetric potentials at critical binding strength do not reflect? [Hint: one counterexample is sufficient to disprove a conjecture. Try a square well.]
2. The Gaussian wave packet  $\Phi_0$  and the  $\nu=1$  wave packet  $\Phi_1$  (Eqs. (25) and (36)) both have shorter wavelengths at the front: see Figs. 3–5. For the Gaussian pulse the phase  $\phi$ , defined by  $\Phi = |\Phi|\exp(i\phi)$ , is

$$\phi(x, t) = k_0 \left( x - x_0 - \frac{1}{2}v_0 t \right) + \frac{(x - x_0 - v_0 t)^2 \hbar t / 2m}{b^4 + (\hbar t / m)^2}. \quad (59)$$

A wavelength can be defined by  $\phi(x + \lambda, t) - \phi(x, t) = 2\pi$ , or  $\phi(x + \lambda/n, t) - \phi(x, t) = 2\pi/n$ . In the limit of large  $n$  we obtain the *local wavelength*

$$\lambda(x, t) = \frac{2\pi}{\partial_x \phi(x, t)}. \quad (60)$$

Verify that for the Gaussian packet Eq. (60) gives

$$\lambda_0(x, t) = \frac{2\pi}{k_0 + \frac{2(x - x_0 - v_0 t)\hbar t / m}{b^4 + (\hbar t / m)^2}}. \quad (61)$$

Find the corresponding result for  $\Phi_1$  and compare with plots of  $\Phi_0$  and  $\Phi_1$ .

3. The phase  $\phi(x, t)$  of a wave packet is stationary when  $d\phi = \partial_x \phi(x, t)dx + \partial_t \phi(x, t)dt$  is zero. The phase velocity is the value of  $dx/dt$  when  $d\phi$  is zero,  $v_p = -\partial_t \phi(x, t) / \partial_x \phi(x, t)$ . Find  $v_p$  for the Gaussian free-space packet, and show that the phase speed is half the group speed ( $v_p = v_0/2$ ) at the center of the packet, where  $x = x_0 + v_0 t$ . Explore the behavior of  $v_p$  for  $\Phi_0$  and for  $\Phi_1$ .
4. The locus of  $[\operatorname{Re} \Phi, \operatorname{Im} \Phi, x]$  is, at a given time, a curve in space. For  $\Phi = e^{ik(x-vt)}$  the curve is a right-handed helix of pitch  $2\pi/k$ , if  $\operatorname{Re} \Phi$ ,  $\operatorname{Im} \Phi$ , and  $x$  form a right-handed coordinate system. A snapshot of the space curve of  $\Phi_1$  is shown in Fig. 5. It is predominantly right handed, but there is a left-handed portion in the tail. The curve is right handed if the phase is increasing with  $x$ ; the change in handedness occurs at zeros of  $\partial_x \phi(x, t)$ . Verify that for the Gaussian packet the change occurs at

$$x = x_0 + v_0 t - \frac{mk_0}{2\hbar t} [b^4 + (\hbar t / m)^2], \quad (62)$$

and find the corresponding result for  $\Phi_1$ . Compare with plots of the space curves.

5. The reflectionless wave packets  $\Phi_1$  in Eq. (36) and  $\Phi'_1$  in Eq. (37) are both characterized by the same parameters  $a$ ,  $b$ ,  $k_0$ , and  $m$ . We saw in Sec. IV that the  $\Phi_1$  wave packet generally has group speed greater than the group speed  $v_0 = \hbar k_0 / m$  of the Gaussian packet  $\Phi_0$ . Is the same true of  $\Phi'_1$ ? Is  $\Phi_1$  or  $\Phi'_1$  faster for the same parameter set?
6. There is a one-to-one correspondence between the reflection of  $s$ -polarized electromagnetic waves and the reflection of particle waves (see, for example, Ref. 12, Sec. 1-3):

$$\varepsilon(x) \frac{\omega^2}{c^2} \leftrightarrow \frac{2m}{\hbar^2} [E - V(x)]. \quad (63)$$

Here  $\varepsilon(x)$  is the dielectric function,  $\omega$  the angular frequency, and  $c$  is the speed of light. Write  $\varepsilon(x) = 1 + \Delta\varepsilon$ , and find the functional form of  $\Delta\varepsilon$  corresponding to the  $V(x)$  given in Eq. (1). Is  $\Delta\varepsilon$  frequency dependent?

<sup>a)</sup>Electronic address: john.lekner@vuw.ac.nz

<sup>1</sup>P. S. Epstein, "Reflection of waves in an inhomogeneous absorbing medium," Proc. Natl. Acad. Sci. U.S.A. **16**, 627–637 (1930).

<sup>2</sup>C. Eckart, "The penetration of a potential barrier by electrons," Phys. Rev. **35**, 1303–1309 (1930).

<sup>3</sup>L. D. Landau and E. M. Lifshitz, *Quantum Mechanics* (Pergamon, Oxford, 1965), 2nd ed., Secs. 23 and 25.

<sup>4</sup>S. Flügge, *Practical Quantum Mechanics* (Springer-Verlag, Berlin, 1974), Problem 39.

<sup>5</sup>I. Kay and H. E. Moses, "Reflectionless transmission through dielectrics and scattering potentials," J. Appl. Phys. **27**, 1503–1508 (1956).

<sup>6</sup>N. Kiriushcheva and S. Kuzmin, "Scattering of a Gaussian wave packet by a reflectionless potential," Am. J. Phys. **66**, 867–872 (1998).

<sup>7</sup>F. Oberhettinger, "Hypergeometric functions," in *Handbook of Mathematical Functions*, edited by M. Abramowitz and I. A. Stegun (NBS Applied Mathematics Series No. 55, 1964), Chap. 15.

<sup>8</sup>E. H. Kennard, "Zur quantenmechanik einfacher bewegungstypen," Z. Phys. **44**, 326–352 (1927).

<sup>9</sup>C. G. Darwin, "Free motion in the wave mechanics," Proc. R. Soc. London, Ser. A **117**, 258–293 (1928).

<sup>10</sup>W. Gautschi, "Error function and Fresnel integrals," in *Handbook of Mathematical Functions*, edited by M. Abramowitz and I. A. Stegun (NBS Applied Mathematics Series No. 55, 1964), Chap. 7.

<sup>11</sup>J. Lekner, "Nonreflecting stratifications," Can. J. Phys. **68**, 738–742 (1990).

<sup>12</sup>J. Lekner, *Theory of Reflection of Electromagnetic and Particle Waves* (Nijhoff/Springer, Dordrecht/Berlin, 1987).

<sup>13</sup>J. Lekner, "Critical binding of diatomic molecules," Mol. Phys. **23**, 619–625 (1972).

<sup>14</sup>F. Cooper, A. Khare, and U. Sukhatme, *Supersymmetry in Quantum Mechanics* (World Scientific, Singapore, 2001), pp. 46–47.

#### ONLINE COLOR FIGURES AND AUXILIARY MATERIAL

AJP uses author-provided color figures for its online version (figures will still be black and white in the print version). Figure captions and references to the figures in the text must be appropriate for both color and black and white versions. There is no extra cost for online color figures.

In addition AJP utilizes the Electronic Physics Auxiliary Publication Service (EPAPS) maintained by the American Institute of Physics (AIP). This low-cost electronic depository contains material supplemental to papers published through AIP. Appropriate materials include digital multimedia (such as audio, movie, computer animations, 3D figures), computer program listings, additional figures, and large tables of data.

More information on both these options can be found at [www.kzoo.edu/ajp/](http://www.kzoo.edu/ajp/).